

Relationships Between Porosity and Permeability for Porous Rocks

Shouxiang Ma¹ and Norman R. Morrow^{1,2}

¹ Western Research Institute, 365 N.9th St., Laramie, WY 82070-3380, USA

² Chemical and Petroleum Engineering Department, University of Wyoming, Laramie, WY 82070, USA

1996 International Symposium of the Society of Core Analysts, Sept. 8-10, Montpellier, France

Abstract

Correlations between porosity, ϕ , and permeability, k , are often tested for sedimentary rocks in relation to petroleum geology and reservoir characterization. A general trend of increase in permeability with porosity can be expected. However, the effects of grain size, packing, compaction, and solution/dissolution processes related to development, preservation or loss of primary and secondary porosity can lead to a wide variety of relationships between permeability and various forms of porosity. In the present work, general relationships have been tested for a very large data set (578 samples). The correlation coefficient for the logarithm of permeability and porosity was $R=0.42$.

In addition to permeability and porosity, the information for this data set included mercury injection capillary pressure, P_C , curves. The Thomeer model was used to fit the P_C curves. The fitted curves were defined by the two parameters of the model: the pore structure factor, G , and the threshold pressure, P_T , given by the model at 100% saturation. This procedure avoids the problem of defining the entry pressure from P_C data especially if there is a knee associated with small or vuggy samples. P_T provides an estimate of the largest connected pore throat size in the high saturation range and G represents the distribution of pore throat sizes with respect to their control of mercury invasion. As G increases, the fraction of the volume of the pore network that is dominant in determining permeability decreases.

Of the 578 samples, P_C data points for 463 samples could be fitted by the Thomeer model with $R \geq 0.85$. Distributions of k , ϕ , P_T , and G are presented for these data sets. The pore structure dependence of k - ϕ correlations is illustrated explicitly in terms of G and P_T . Permeability correlated strongly with P_T ($R=0.82$). This correlation was improved by including ϕ ($R=0.87$), and further improved by including G ($R=0.93$). The Swanson parameter, $\phi(S_N/P_C)_{MAX}$, which includes ϕ , P_T , and G implicitly and is obtained directly from the measured P_C curves, gave the best correlation ($R=0.95$). Application of the curve fitting parameters demonstrates the advantages and disadvantages of fitting experimental data to mathematical models for the purpose of developing generalized correlations of petrophysical data.

INTRODUCTION

Tests of petrophysical data for correlations between porosity, ϕ , and permeability, k , are very common in geological and engineering applications (Nelson, 1994). However, it is possible that a core sample has fairly low porosity but may have relatively high permeability such as the Ste. Genevieve

oolid grainstone formation (Choquette and Steiner, 1985). Alternatively, core samples can have extremely high porosity with very low permeability as in many types of carbonate rocks such as the North Sea chalk ($\phi > 40\%$, $k < 10$ md; Spinler and Hedges, 1995) and the California diatomites ($\phi > 60\%$, $k < 3$ md; Koh et al., 1996). Permeability is proportional to the square of pore throat size. Thus, the larger connected pore throats, represented by threshold pressure, P_T , dominate the permeability. Porosity is directly proportional to the volume of both pore bodies and throats, but is usually dominated by pore bodies. On the other hand, the diagenetic processes occurring in sedimentary rocks can cause change in porosity and interrelated changes in the size of both pore bodies and throats (Coskun et al., 1993). In addition, permeability can be strongly dependent on direction of flow whereas porosity is a global property. Therefore correlations between ϕ and k are observed but they are strongly dependent on pore structure.

Besides threshold pressure and porosity, the pore throat size distribution, as indicated by capillary pressure, P_C , curve shape, also affects permeability because it is the distribution of pore throats that determines how much pore volume is accessed by macro-pore throats (in the low nonwetting phase saturation, S_N , range) and how much is accessed by micro-pore throats (in the high S_N range). Therefore, prediction of permeability requires information on threshold pressure, porosity, and pore throat size distribution.

Permeability Predictions - A Brief Review

Many correlations between permeability, k , and other petrophysical properties have been reported. Purcell (1949) presented a method of obtaining mercury injection P_C curves for core samples and derived a relationship between permeability and P_C curves. Data measured on 27 samples verified the method. A lithology factor was introduced to compensate for the differences in pore structure between different formations.

Mercury injection data is now widely used to obtain information on pore structure. Pore throat size distribution, pore connectivity, ϕ , and P_T can be derived from these measurements. Thomeer (1960) showed that P_C data could be fitted satisfactorily with an empirical equation,

$$\log \left(\frac{P_C}{P_T} \right) \log S_N = -G^2 \quad (1)$$

where G is a pore structure factor determined by P_C curve

shape. By plotting k vs ϕ/P_T for a data set of 144 samples, Thomeer found a fairly good correlation for samples with similar G . In fitting a larger data set of 279 samples, Thomeer (1983) included G and obtained a improved correlation with permeability. Through percolation theory, Katz and Thompson (1986) presented a similar $k-\phi/P_T$ correlation where P_T is the percolation threshold which was defined as the inflection point at the low S_N range of the P_c curves.

Swanson (1981) noted that the 45° tangent point, point A, to the Thomeer P_c curves corresponds to the region of change in slope of the residual-initial nonwetting phase saturation relationship (Pickell et al., 1966). The value of S_N at point A was considered to correspond to the effective volume that controls permeability. A total of 319 samples were used to establish relationships between permeability and properties derived from point A. Based on the work of Thomeer (1960) and Swanson (1981), Pittman (1992) analyzed 202 samples in order to correlate permeability, porosity, and pore aperture size (a property which is inversely proportional to capillary pressure and is extremely important in evaluating seals as traps and in explaining the locations of stratigraphic hydrocarbon accumulations).

Kamath (1992) analyzed the different methods of predicting permeability from P_c curves for 158 samples. The analysis also included results for 268 samples from Swanson (1981), 29 from Walls and Amæfule (1985), and 47 from Thompson et al. (1987). $k=1$ md was used as a cut-off for division of the data into two groups. Kamath concluded that the Swanson method gives the best prediction of permeability from P_c measurements.

Database and Objectives of This Study

A total of 578 data sets that included measurements of mercury injection P_c curves, k , and ϕ were used in the present study. Of the 578 P_c curves, 463 fitted the Thomeer model (Eq. 1) with a correlation coefficient $R \geq 0.85$. Both P_T and G were calculated for the 463 samples. Detailed analysis of the model and the 578 data sets are available (Ma, 1992). The samples originated worldwide from both sandstone and carbonate formations and include the data sets of Kamath (1992). Data for other published correlations were not available.

The main objective of the present study was to test correlations between k , ϕ , P_T , and G for the 463 samples. Capillary pressure curves were mathematically modeled by using the Thomeer model with a computer algorithm for curve fitting and determination of the parameters (ϕ , P_T , and G). The effect of these parameters on $k-\phi$ correlations was examined in detail. The best model, based on the data base, of predicting permeability from ϕ , P_T , and G was identified.

BACKGROUND

Porosity and Permeability

Porosity. Porosity has been classified by Lucia (1995) as interparticle and vuggy. Interparticle porosity includes intergrain and/or intercrystal porosities and correlates reasonably well with permeability. Porosity identified as

vuggy, which may include separate vugs and fractures, does not correlate with permeability.

Porosity of porous media is defined as, $\phi = V_p/V_b$, where V_p is the pore volume and V_b the bulk volume. Conceptually, if V_p =total pore volume, the porosity is the total porosity. If V_p =effective pore volume, the porosity is the effective porosity. Obviously, the effective porosity will correlate better with permeability than the total porosity. However, the difference between the total and effective porosities is generally very small for sedimentary rocks and will be neglected.

For a core sample of bulk volume V_b , porosity is proportional to the pore volume. Although all the pore bodies and their throats contribute to porosity, pore bodies (because of their size) play a much more important role than the pore throats.

Permeability. Permeability is defined by Darcy's law,

$$k = \frac{q \mu L}{A \Delta P} \quad (2)$$

where q is the flow rate, μ the fluid viscosity, L the length, A the cross sectional area of the sample, and ΔP the pressure drop. Permeability is commonly related to pore size through the Poiseuille equation for a parallel bundle of tubes,

$$q = \frac{n \pi r^4 \Delta P}{8 \mu L} \quad (3)$$

where n is the number and r the radius of the tubes. Because $A = n\pi r^2/\phi$, combination of Eqs. 2 and 3 gives

$$k = \frac{\phi r^2}{8} = \frac{\phi d^2}{32} \quad (4)$$

or

$$r_M = \sqrt{\frac{8k}{\phi}} \quad (5)$$

where d is the tube diameter and r_M the microscopic pore size (Leverett, 1939). Eq. 4 shows that permeability is proportional to pore size squared.

Fig. 1 illustrates three simple pore/throat systems. Fig. 1a shows a cylindrical pore of diameter d inside a solid cylindrical matrix of diameter D with d/D being 0.1. The pore volume of this system is $\pi d^2 L/4$ and the porosity is $\phi_{1A} = d^2/D^2 = 1\%$. The permeability (entrance and exit effects are neglected) is $k_{1A} = d^4/(32D^2) = d^2/3200$.

Fig. 1b shows a pore body (diameter d_p and length L_p) and two pore throats (diameter d_T). For cylindrical tubes of different sizes, connected in series, the generalized forms of

porosity and permeability are respectively,

$$\phi_{1B} = \frac{d_T^2}{D^2} \left(\frac{L_P}{L} \frac{d_P^2}{d_T^2} + 1 - \frac{L_P}{L} \right) \quad (6)$$

and

$$k_{1B} = \frac{d_T^4}{32 D^2 \left(\frac{L_P}{L} \frac{d_T^4}{d_P^4} + 1 - \frac{L_P}{L} \right)} \quad (7)$$

With the dimensions shown in Fig. 1b, i.e., $L_P/L=0.8$ and $d_P/d_T=6$, porosity and permeability expressed by Eqs. 6 and 7 are $\phi_{1B} = (28.8 + 0.2)d_T^2/D^2$ and

$$k_{1B} = \frac{d_T^4}{32 D^2 \left(0.2 + \frac{0.8}{1296} \right)}$$

These two expressions indicate that the pore body contributes 99.31% of the total porosity but determines only 0.31% of the total permeability. On the other hand, the two pore throats contribute 0.69% of the total porosity but control 99.69% of the total permeability. If $\phi_{1B} = \phi_{1A}$, then $d_T = d/\sqrt{29}$ and $k_{1A} \approx 169k_{1B}$.

Fig. 1c shows another pore body and two pore throats with $L_P/L=0.8$ and $d_P/d_T=6$. The permeability in this case, k_{1C} , can also be expressed by Eq. 7. Let $k_{1C} = k_{1A}$, then $d_T \approx 0.6693d$. The porosity from Eq. 6 is $\phi_{1C} = 13\% = 13\phi_{1A}$.

These simple examples show that it is easy to construct configurations that can have the same porosity, but very different permeabilities, or the same permeability, but greatly different porosities. The essential difference between these configurations is pore structure.

Sample Size

Information on formation permeability is sometimes obtained from P_c measurements on drill cuttings. This is especially useful if core samples are not available. However, there is still a problem. The small size of even the largest drill cuttings (about 10 mesh or 2.5 mm particle diameter; Bush and Freeman, 1986) may affect the measured P_c curves because of the effective increase in connectivity related to the high surface to volume ratio. This effect depends on sample geometry and pore throat size. The influence of the fraction of exterior surface open to invasion has been calculated by Mason and Mellor (1991) for random sphere packs.

A characteristic length, L_c , applied to scaling of spontaneous imbibition measurements (Ma et al., 1995a), provides a linear measure of effective sample size,

$$L_c = \sqrt{\frac{V_B}{\sum_{i=1}^n \frac{A_i}{l_{A_i}}}} \quad (8)$$

Where A_i is the area perpendicular to the i th imbibition direction and l_{A_i} the distance from A_i to the no-flow boundary. V_B can be measured and A_i and l_{A_i} can be estimated for drill cuttings.

Decrease in L_c by a factor of $2/\pi$ unifies simulation results (Lim and Aziz, 1995) for prediction of single phase flow. At the present state of knowledge, definition of the characteristic length as $L_{c,s} = 2L_c/\pi$ provides the best estimate of a physically significant characteristic length for various shapes and boundary conditions. $L_{c,s}$ could be of broad value with respect to a variety of mass and heat transfer processes.

The Leverett microscopic radius (Eq. 5) provides correlation of spontaneous imbibition results for several types of strongly water-wet porous media (Ma et al., 1995b). The ratio of $L_{c,s}$ to r_m provides a dimensionless measure, N_r^L , of sample size to microscopic length for samples of different permeability, porosity, size, shape and boundary conditions.

$$N_r^L = \frac{L_{c,s}}{r_m} \quad (9)$$

Capillary pressure measurements will become increasingly sensitive to decrease in sample size below a critical value of N_r^L . For a Berea Sandstone core ($k=500$ md and $\phi=20\%$; $r_m=4.4 \mu\text{m}$) having dimensions that are typical for mercury injection measurements (say $d=3.81$ cm and $L=1$ cm), $L_{c,s}=2984 \mu\text{m}$ and $N_r^L=678$. For a cube with size length of 2.5 mm, $L_{c,s}=459 \mu\text{m}$ and for $r_m=4.4 \mu\text{m}$, $N_r^L=104$. The problem of accuracy in P_c data measurement of small volume can, of course, be reduced by using a sufficient number of cuttings.

Severe effects of sample size on capillary pressure data for bead packs and rock samples can be avoided if the sample thickness is greater than about 10 particle diameters (Larson and Morrow, 1981; Thompson et al., 1987). For bead packs this corresponds to $N_r^L \approx 50$, which implies that sample size effect would not be serious for rocks of less than about 2000 md permeability. (A cube with $a=2.47$ mm, $\phi=20\%$, and $N_r^L=50$ will have $k=2088$ md). The effective characteristic length of rock chips can be increased by sealing off a large fraction of the surface. For example, $L_{c,s}$ for a cube is increased by a factor of 3.5 if only one side of the cube is open to invasion.

In summary, N_r^L provides a useful method of gauging the likely sensitivity of capillary pressure data to sample size. In the present study, N_r^L is assumed to be much larger than 50 and that the sample sizes are more than adequate.

Characterization of Pore Structure

Pore structure determines the relationships between porosity and permeability. Characterization of pore structure is one of the most important tasks in petrophysics. Thin sections provide essentially a two-dimensional view of the complicated three-dimensional pore structures of porous media. Methods of estimating porosity and permeability from two-dimensional thin sections have been proposed (Ehrlich and Davies, 1989).

Pore structure information derived from mercury injection P_c curves is essentially three-dimensional. Ma and Morrow (1993) identified four operational definitions of similar pore structures from P_c curves. Systems with the same pore size distribution (or the same G factor) have identical $J-S_N$ curves, where $J = P_c \sqrt{k/\phi}/\sigma$. However, systems with the same $J-S_N$ curves can be divided into four different groups with each characterized by different petrophysical properties. For statistically identical, pseudo-identical, and pseudo-similar systems, as defined by Ma and Morrow (1993), correlations may exist between porosity and permeability. For geometrically similar systems, such as random packings of equal spheres (diameter d_s), there is no correlation between permeability and porosity. Porosity is essentially constant (~37%), $P_T \propto 1/d_s$ and $k \propto d_s^2 \propto 1/P_T^2$ (Morrow et al., 1969).

For packings of variable porosity, the Kozeny equation indicates the dependence of permeability on porosity and particle size,

$$k = \frac{d_s^2}{36 K_z} \frac{\phi^3}{(1-\phi)^2} \quad (10)$$

where K_z is the Kozeny constant, which is about 5 for packings of equal sized particles (Dullien, 1992).

RESULTS AND DISCUSSION

Distribution of Petrophysical Properties

The number distributions of porosity and logarithm of permeability are shown in Figs. 2a and 2b respectively for the 578 data sets. Permeabilities in the range of 1-1000 md are the most frequent; porosities are in the range 12 to 24%, peaking at 19%. Both distributions are close to normal. This appears to support the conclusions reached by Freeze (1975) that the porosity and the logarithm of permeability should correlate.

Distributions of threshold pressure and pore structure factor were obtained by fitting the measured P_c curves with the Thomeer model (Eq. 1). Data which fit the model with a correlation coefficient ≥ 0.85 (total of 463 samples or 80% of the total 578 samples) are shown in Figs. 2c and 2d, respectively. The threshold pressure mode is about 0.5 bar; pore structure factor has a mode of about 0.4.

Permeability vs Porosity

For the 578 data sets (data will be referred to by the number of samples in the set), the correlation between permeability and porosity is shown in Fig. 3 (correlation coefficient $R=0.4180$). Hypothetical solutions to the Kozeny equation (Eq. 10) relating permeability to porosity and

particle size are also shown in Fig. 3. (The Kozeny equation was developed for unconsolidated porous media.) The particle size which fits the average trend between permeability and porosity is about $d_s=20 \mu\text{m}$. This is about 5 times smaller than typical particle sizes for consolidated sandstones. Thus prediction of permeability from the particle sizes of consolidated porous media through application of the Kozeny equation will require some form of adjustment factor which is difficult to determine or even identify physically.

Fig. 3 can be divided into three regions. In the high porosity Region I ($\phi > 28\%$), there is basically no correlation between permeability and porosity. This is probably because the high porosity porous media are probably either carbonates or unconsolidated sands. Carbonates tend to have separated vugs and vuggy porosity does not correlate with permeability. For well sorted unconsolidated sands, the porosity is high and independent of particle size, while permeability is proportional to the particle size squared.

Formations with low porosity (Region III, $\phi < 5\%$) are usually of no practical interest with respect to oil production (Hilchie, 1982). The permeabilities of systems with $\phi < 5\%$ are usually less than 0.1 md. Accurate measurements of permeability below this value are not usually made in routine core analysis related to oil recovery. Porosity values for cores below 5% are often reported as being less than some selected cut-off value. A total of 67 samples have $\phi > 28\%$ or $\phi < 5\%$. The correlation between k and ϕ for the remaining 511 data sets (Region II) is $R=0.5935$.

Effect of pore structure factor. For the 463 data sets for which the P_c curves fitted the Thomeer model with $R \geq 0.85$ (see Fig. 4a), the quality of the correlation between permeability and porosity is almost the same as that for the 578 data sets.

The effect of pore throat size distribution on $k-\phi$ correlations has been studied by subdividing the 463 data sets based on the values of G . For the small number of samples with $G < 0.1$, either the porous media has a very narrow pore throat size distribution or a few pore throats control most of the porosity such as in vuggy systems. The latter reason may be why permeability tends to decrease with increase in porosity (Fig. 4b). Basically, no $k-\phi$ correlation exists or the correlation is very poor for samples with $G < 0.3$ (Figs. 4b and 4c). This is because threshold pressure controls permeability in this range of G . The effect of smaller pore throats on permeability is insignificant. With increase in G , the contribution to permeability from the pores of different sizes increases and the correlation between k and ϕ improves (Figs. 4d-4g). Fig. 4h shows the $k-\phi$ correlation for all data with $G > 0.3$. (Solid diamond symbols shown in Fig. 4, a total of 6 out of 463 data points were excluded from the analysis because they were well removed from the general trend.)

Porous media with extremely high aspect ratios. Most of the samples with $\phi > 28\%$ (see region I in Fig. 3) have G factors in the range of 0.1-0.3 (Fig. 4). This is expected for unconsolidated systems but not for heterogenous carbonates.

The latter have extremely high aspect ratios and information on pore size distribution, or the G factor, derived from drainage P_C curves may be misleading because access to most of the larger pores is controlled by small pore throats. Heterogeneous pore systems can appear to be homogeneous for this extreme case. Such situations should be readily identified from back-up studies of thin sections.

Effect of threshold pressure. The data sets can also be divided, based on the value of threshold pressure, P_T , as shown in Fig. 5. In each range of P_T , the $k-\phi$ correlation is fairly good. Fig. 5g summarizes these correlations. From this figure, it can be seen that, at any porosity, permeability decreases with increase in threshold pressure.

Permeability vs Threshold Pressure

As discussed above, permeability is proportional to the square of pore throat size. Thus, the larger connected throats are much more important than the smaller ones in determining permeability. The contribution of the largest pore throats to permeability is inversely proportional to the threshold pressure. Thus, there is a strong correlation between permeability and threshold pressure (see Fig. 6a) for the 463 data sets ($R=0.8202$).

The quality of this type of correlation is best for porous media with small G factors. Fig. 6b shows the correlation for samples, 90 in all, with $G<0.2$. The correlation coefficient ($R=0.9246$) is much better than that shown in Fig. 6a. (The correlation parameters a and b represent the intercept at $P_T=1$ bar and the slope of the correlation, respectively). As the pore throat size distribution widens, the correlation between permeability and threshold pressure degrades because the contribution to total permeability by the pore throats with different sizes increases (see Figs. 6c-6e). The trend does not hold for $G>0.8$, but there were only nine samples in this category and the value of R is only slightly higher than for the samples with $0.6 < G < 0.8$.

Correlations of $k-P_T$ for subsets of data based on G are summarized in Fig. 6g. From this figure, it can be seen that k increases, at a given value of P_T , with decrease in G . This relationship is clearly demonstrated by plotting the intercept, a , vs the mid-values of G intervals as shown in Fig. 6h. The absolute value of b decreases linearly with increase in G up to $G=0.8$. This means that the sensitivity of permeability to threshold pressure decreases as the pore size distribution widens. This is consistent with the increased contribution from pore throats of different sizes to permeability with increase in pore structure heterogeneity.

Other Two Parameter Correlations

The 463 sets of data were analyzed in detail by cross-plotting all combinations of the four parameters (k , ϕ , P_T , and G). The following is a brief summary of the observations.

Permeability vs pore structure factor. From Fig. 6g, it can be seen that permeability and pore structure factor correlates for constant threshold pressures. The $k-G$ cross plots show

that the correlations are good for low values of P_T , but become weaker for samples with $P_T > 5$ bars, and even more so for $P_T > 20$ bars.

Porosity vs threshold pressure. As rocks from a common source are compacted and undergo other diagenetic changes that reduce porosity, the reduction in largest connected pore throat size will be reflected by increase in threshold pressure. A general trend of increase in threshold pressure with decrease in porosity was observed for the 463 data sets. When the data sets were subdivided, based on the G factor, no correlation was observed for samples with $G < 0.3$, but weak correlations were observed for $G > 0.3$.

Porosity vs pore structure factor. Theoretically, pore structure factor should not depend on porosity because the pore structure factor is a measure of pore throat size distribution, not the size of pore throats, while porosity is mainly determined by pore bodies. However, porous media with uniform pore structure tend to have higher porosity (such as unconsolidated sands) than those with non-uniform pore structure. The 463 data sets show that G factor decreases with increase in porosity.

The data sets were subdivided based on P_T . Correlations for P_T -based data subsets were no better than for the original 463 data sets. For samples with $P_T > 5$ bars (very small pore throats), the G factor was independent of the porosity.

Threshold pressure vs pore structure factor. From analysis of the 463 data sets, rocks with higher pore structure factors tended to have lower threshold pressures. This may result from a tendency for the largest pore throats to be linked in rocks with uniform pore structure.

In summary, the correlations between permeability, porosity, pore structure factor, and threshold pressure all indicate that sedimentary rocks tend to have correlatable pore size, pore throat size, and pore throat size distribution.

Multi-parameter Correlations of Permeability

Katz-Thompson correlation. Through percolation theory, Katz and Thompson (1986) derived an equation relating permeability to porosity and threshold pressure. This relationship is shown in Fig. 7a for the data set of 463 samples (correlation coefficient $R=0.8727$). This is much better than the $k-\phi$ correlation ($R=0.4147$, Fig. 4a) and is a distinct improvement over the $k-P_T$ correlation ($R=0.8202$, Fig. 6a). This is because threshold pressure relates to pores that make a dominant contribution to total permeability, whereas porosity contains information on both macro- and micro-pores. The combination of threshold pressure and porosity thus gives a better prediction of permeability than either threshold pressure or porosity alone.

The Thomeer correlation. As discussed above, permeability is influenced by pore throat size distribution represented by the G factor. Addition of G to the correlating group should give a better prediction of permeability than threshold

pressure and porosity alone. Thomeer (1983) proposed the following correlation for prediction of permeability,

$$k \propto \left(\frac{\phi}{P_T G^{1.334}} \right)^2 \quad (11)$$

This relationship implies that permeability decreases with increase in pore structure factor. For the 463 data sets, the Thomeer correlation (Fig. 7b, $R=0.9294$) is much better than the $k \sim \phi/P_T$ correlation (Fig. 7a).

The Swanson correlation. Swanson (1981) proposed a method of correlating permeability with the portion of pore volume considered to be most effective in determining permeability. The effective pore volume identified with the tangent point for an angle of 45° on the Thomeer plot. Based on the solutions derived by Ma et al. (1991), the Swanson parameter can be expressed analytically by the three Thomeer parameters.

$$\left(\frac{S_B}{P_C} \right)_{45^\circ} = \phi \left(\frac{S_N}{P_C} \right)_{45^\circ} = \frac{\phi}{P_T 10^{2G}} \quad (12)$$

Comparison of Eqs. 11 and 12 shows that the only difference between the two expressions is the exponent of the pore structure factor. The correlation between permeability and the analytical Swanson parameter is shown in Fig. 7c ($R=0.9362$); this is a slight improvement over the Thomeer correlation.

Based on Walls and Amæfule (1985), Ma (1992) used a method of identifying the Swanson parameter by picking the maximum of S_B/P_C or S_N/P_C rather than matching the Thomeer model. A subroutine was developed to process the 578 samples. The correlation between permeability and the Swanson parameter, $\phi(S_N/P_C)_{MAX}$, is shown in Fig. 7d ($R=0.9515$ for the 463 data sets) and in Fig. 8a ($R=0.9432$ for the 578 data sets).

The relationship between permeability and the Swanson parameter for the 463 samples is

$$k = 376 \left(\frac{\phi S_N}{P_C} \right)_{MAX}^{1.54} \quad (13)$$

where k is in md, P_C is in psi, and ϕ and S_N are fractions.

From Fig. 8a, it can be seen that data are scattered for samples with $k < 10$ md. Thus $k=10$ md was used as a cut-off to divide the 578 data sets. The correlation coefficient for samples with $k > 10$ md, shown in Fig. 8b, is only slightly better than the correlation for the 578 data sets, but should provide closer prediction for rocks in the high permeability range.

Overall, the Swanson parameter performs better than the Thomeer parameter. Hagiwara (1986) found that the Swanson parameter could be further improved by including an exponent, the Archie cementation exponent, on porosity and

nonwetting phase saturation. An optimal exponent can be determined which gives the best correlation. However, the values of the exponent varied when tested for different data sets and the correlations were only slightly improved (Ma, 1992).

In summary, all forms of the Thomeer and Swanson parameters, which include porosity, threshold pressure, and pore structure factor either explicitly or implicitly predict permeability satisfactorily. The difference in performance between the parameters probably results mainly from the deviation from the experimental results that arises in fitting data to the Thomeer model. Fitting measured data to a mathematical model enables systematic analyses. The slight reduction in quality of the correlation is minor compared to the advantages of having mathematical descriptions of the P_c curves. This study provides strong support for using the method as proposed by Swanson for a general correlation of permeability with capillary pressure measurements.

CONCLUSIONS

Examination of a very large set of permeability, porosity, and capillary pressure data showed that weak correlations exist between (1) permeability and porosity, (2) permeability and pore structure factor, (3) porosity and threshold pressure, (4) porosity and pore structure factor, and (5) threshold pressure and pore structure factor. A strong correlation was observed between permeability and threshold pressure. Much improved correlations can be obtained between permeability and porosity, threshold pressure, or pore structure factor, if the data set is subdivided based on either pore structure factor or threshold pressure. Overall, the Swanson and the Thomeer parameters predict permeability satisfactorily. The distinct advantages, with respect to analysis of large data sets, of obtaining parametric descriptions of capillary pressure data, such as given by the Thomeer model, far outweigh the disadvantage of minor loss of quality of correlation.

ACKNOWLEDGMENT

We thank ELF, Chevron, Statoil, and NorskHydro for contribution of data. This work was supported by Arco, British Petroleum, Chevron, Conoco, Dagang, ELF, Exxon, Mobil, NorskHydro, Phillips, Shell, Statoil, Unocal, the Western Research Institute Jointly Sponsored Research Program, and the Enhanced Oil Recovery Institute of the University of Wyoming.

REFERENCES

- Bush, D.C. and Freeman, D.L. (1986): "Drill Cuttings Porosity, Grain Density, and Permeability by Direct Laboratory Measurements and Their Reliability," SPWLA 27th Annual Logging Symp., June 9-13.
- Choquette, P.W. and Steiner, R.P. (1985): "Mississippian Oolite and Non-Supratidal Dolomite Reservoirs in the Ste. Genevieve Formation, North Bridgeport Field, Illinois Basin," in P.O. Roehl and P. Choquette, eds., *Carbonate Petroleum Reservoirs*, Springer-Verlag, 209-38.
- Coskun, S.B., Wardlaw, N.C., and Haverslew, B. (1993): "Effect of Composition, Texture and Diagenesis on Porosity, Permeability, and Oil Recovery in a Sandstone Reservoir," *JPS&E*, 8, 279-92.
- Dullien, F.A.L. (1992), *Porous Media - Fluid Transport and Pore Structure*, Academic Press, Inc, San Diego (p.256).
- Ehrlich, R. and Davies, D.K. (1989): "Image Analysis of Pore Geometry: Relationship to Reservoir Engineering and Modeling," paper SPE 19054, SPE Gas Tech. Symp., Dallas, TX, June 7-9.
- Freeze, R.A. (1975): "Analysis of One-Dimensional Ground Water Flow in a Non-Uniform Homogeneous Medium," *Water Resources Research*, v.11, 725-41.
- Hagiwara, T. (1986): "Archie's M for Permeability," *The Log Analyst* (Jan.-Feb.) 39-42.
- Hilchie, D.W. (1982), *Applied Openhole Log Interpretation for Geologists and Engineers*, D.W. Hilchie Inc., CO.
- Kamath, J. (1992): "Evaluation of Accuracy of Estimating Air Permeability from Mercury Injection Data," *SPEFE* (Dec.) 304-10.
- Katz, A.J. and Thompson, A.H. (1986): "Quantitative Prediction of Permeability in Porous Rock," *Physical Review B*, v.34, 8179-81.
- Koh, C.J., Dagenais, P.C., Larson, D.C., and Murer, A.S. (1996): "Permeability Damage in Diatomite Due to In-Situ Silica Dissolution/Precipitation," paper SPE 35394, SPE/DOE 10th Symp. on IOR, April 21-24, Tulsa, OK.
- Larson, R.B. and Morrow, N.R. (1981): "Effects of Sample Size on Capillary Pressures in Porous Media," *Powder Technology*, v.30, 123-38.
- Leverett, M.C. (1939): "Flow of Oil-Water Mixtures Through Unconsolidated Sands," *Trans AIME*, v.132, 149.
- Lim, K.T. and Aziz, K. (1995): "Matrix-Fracture Transfer Shape Factor for Dual-Porosity Simulators," *JPS&E*, 13, 169-78.
- Lucia, F.J. (1995): "Rock-Fabric/Petrophysical Classification of Carbonate Pore Space for Reservoir Characterization," *AAPG Bull*, v.79, (Sept) 1275-300.
- Ma, S., Jiang, M., and Morrow, N.R. (1991): "Correlation of Capillary Pressure Relationships and Calculation of Permeability," paper SPE 22685, *the 66th SPE ATCE*, Dallas, TX, Oct. 6-9.
- Ma, S. (1992), *Correlation of Capillary Pressure Relationships and Prediction of Petrophysical Properties of Porous Media*, PhD Dissertation, New Mexico Tech.
- Ma, S. and Morrow, N.R. (1993): "Similarity of Pore Structure and the Selection of Core Samples for Tests of Scaling," Proc. 9th Wyoming Enhanced Oil Recovery Symp., May 12-13, Casper, WY.
- Ma, S., Zhang, X., and Morrow, N.R. (1995a): "Influence of Fluid Viscosity on Mass Transfer between Rock Matrix and Fractures," paper CIM 95-94, Proc. the Petr. Soc. of CIM 46th ATM, May 14-17, Banff, Alberta.
- Ma, S., Morrow, N.R., and Zhang, X. (1995b): "Generalized Scaling of Spontaneous Imbibition for Strongly Water-Wet Systems," paper CIM 95-138, Proc. the 6th Saskatchewan Petr. Conf., Oct. 16-18, Regina.
- Mason, G. and Mellor, D.W. (1991): "Analysis of the Percolation Properties of a Real Porous Material," F. Rodriguez-Reinoso et al. (eds.), *Characterization of Porous Media II*, Elsevier Sci. Pub.
- Morrow, N.R., Huppler, J.D., and Simmons, III, A.B. (1969): "Porosity and Permeability of Unconsolidated, Upper Miocene Sands from Grain-Size Analysis," *J Sedimentary Petrology*, v.39, n.1, 312-21.
- Nelson, P.H. (1994): "Permeability-Porosity Relationships in Sedimentary Rocks," *The Log Analyst* (May-June) 38-62.
- Pickell, J.J., Swanson, B.F., and Hickman, W.B. (1966): "Application of Air-Mercury and Oil-Air Capillary Pressure Data in the Study of Pore Structure and Fluid Distribution," *SPEJ* (March) 55-61.
- Pittman, E.D., (1992): "Relationship of Porosity and Permeability to Various Parameters Derived from Mercury Injection - Capillary Pressure Curves for Sandstone," *AAPG Bull.*, v.76, no.2, 191-198.
- Purcell, W.R. (1949): "Capillary Pressures - Their Measurement Using Mercury and the Calculation of Permeability Therefrom," *Trans AIME*, v.186, 39-48.
- Spinler, E.A. and Hedges, J.H. (1995): "Variations in the Electrical Behavior of the Ekofisk Field in the North Sea," paper SCA 9516, Int. Symp. Of the SCA, San Francisco, CA, Sept. 12-14.
- Swanson, B.F., (1981): "A Simple Correlation between Permeabilities and Mercury Capillary Pressures," *JPT* (Dec.) 2498-504.
- Thomeer, J.H.M. (1960): "Introduction of a Pore Geometrical Factor Defined by the Capillary Pressure Curve," *JPT*, (March) 73-77.
- Thomeer, J.H.M. (1983): "Air Permeability as a Function of Three Pore-Network Parameters," *JPT*, (April) 809-814.
- Thompson, A.H., Katz, A.J., and Krohn, C.E. (1987): "The Microgeometry and Transport Properties of Sedimentary Rock," *Advances in Physics*, v.36, no.5, 625-94.
- Walls, J.D. and Amæfule, J.O. (1985): "Capillary Pressure and Permeability Relationships in Tight Gas Sands," paper SPE 13879, SPE Low Permeability Reservoirs Symp., Denver, May 19-22.

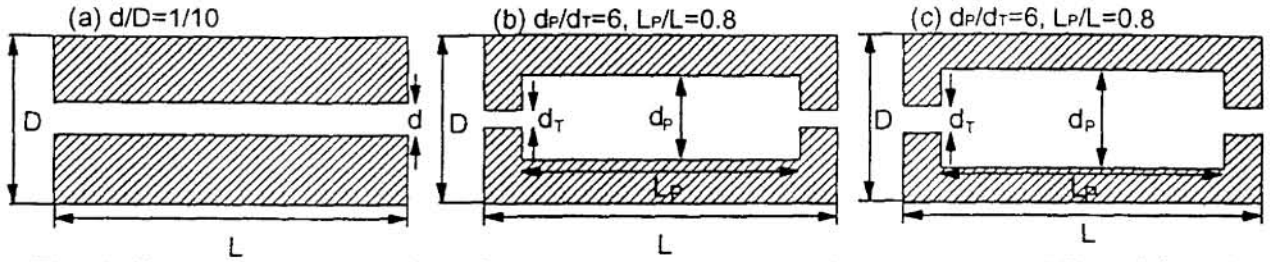


Fig. 1 Illustration of the effect of pore structure on porosity and permeability. (a) a simple cylindrical pore, (b) a pore/throat geometry which has the same porosity as (a), but k decreased by a factor of 169 ($d_T=0.1857d$), and (c) a pore/throat geometry which has the same permeability as (a), but porosity increased by a factor of 13 ($d_T=0.6693d$).

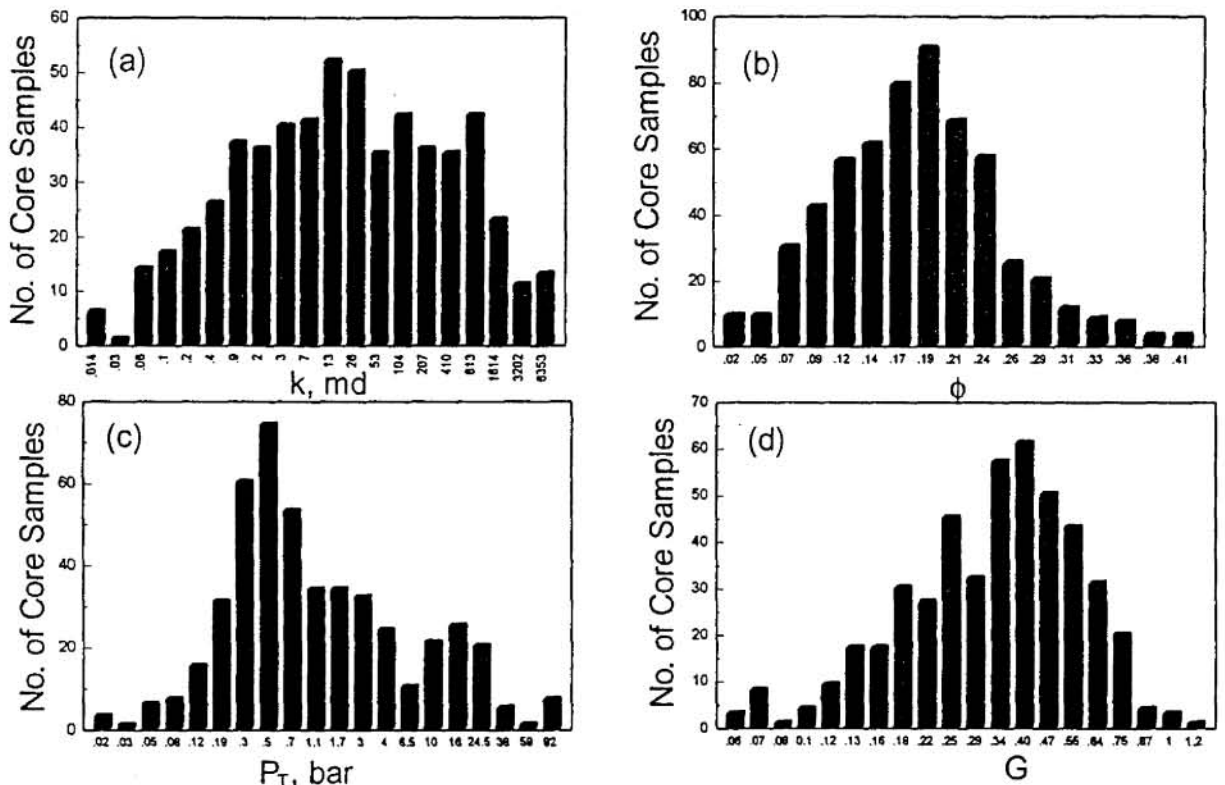


Fig. 2 Distributions of (a) logarithm of permeability and (b) porosity for the data set of 578 samples and distributions of (c) threshold pressure and (d) pore structure factor for the data set of 463 samples fitted by the Thomeer model.

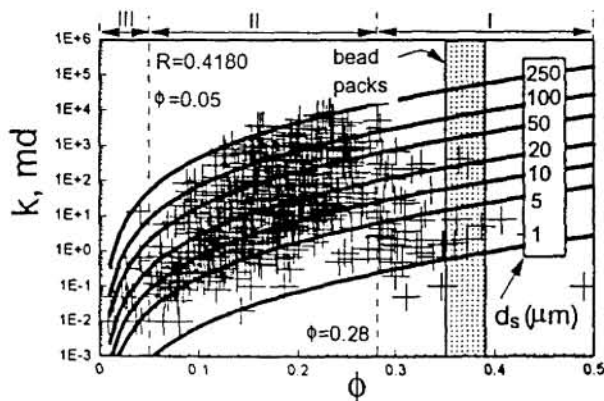


Fig. 3 Correlation between permeability and porosity for the data set of 578 core samples and hypothetical relationships between permeability, porosity, and particle size, d_s , predicted by the Kozeny equation.

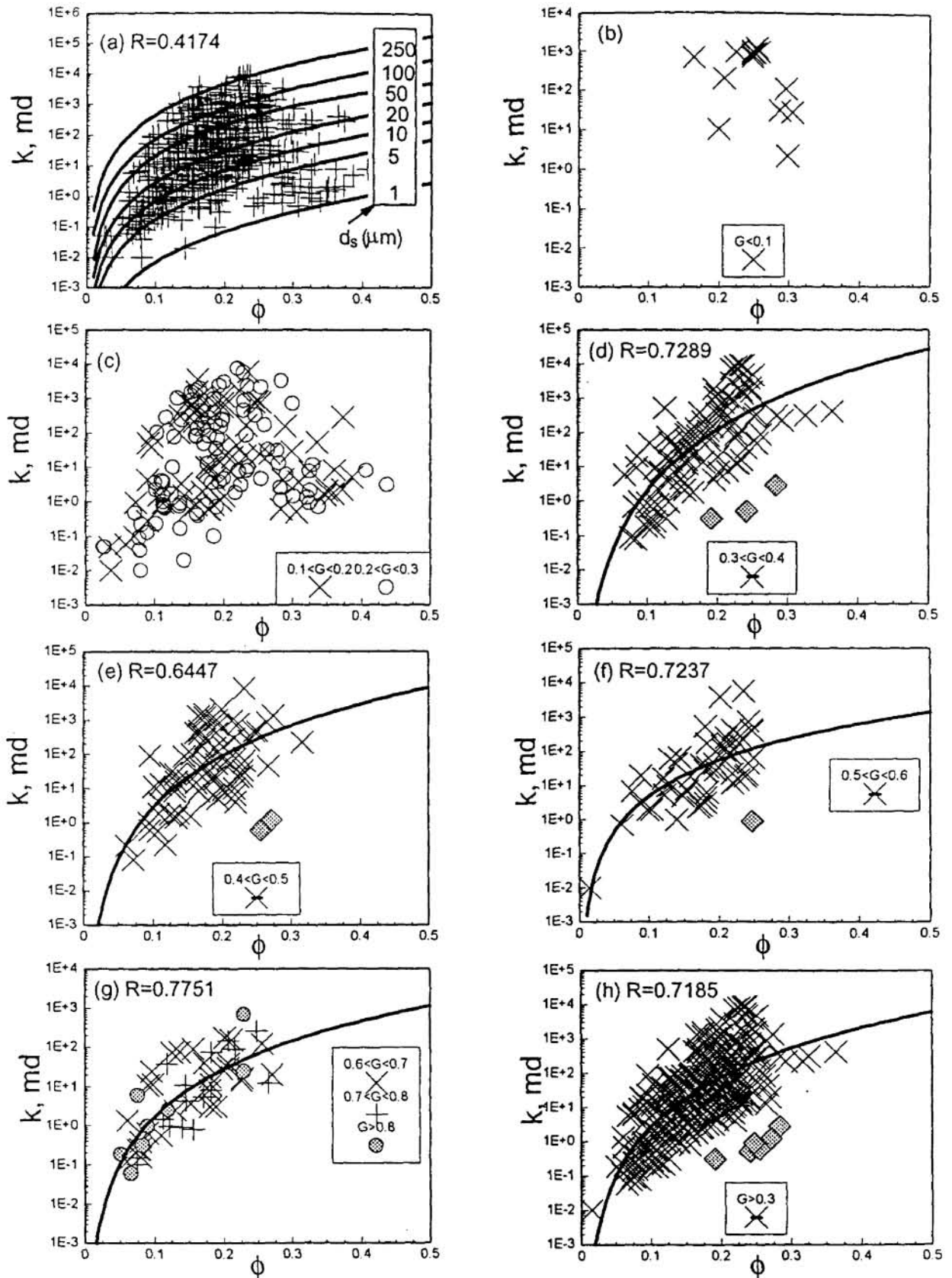


Fig. 4 Correlation between permeability and porosity (a) for the 463 data sets and for data with (b) $G < 0.1$, (c) $0.1 < G < 0.3$, (d) $0.3 < G < 0.4$, (e) $0.4 < G < 0.5$, (f) $0.5 < G < 0.6$, (g) $G > 0.6$, and (h) $G > 0.3$. (\diamond : data excluded.)

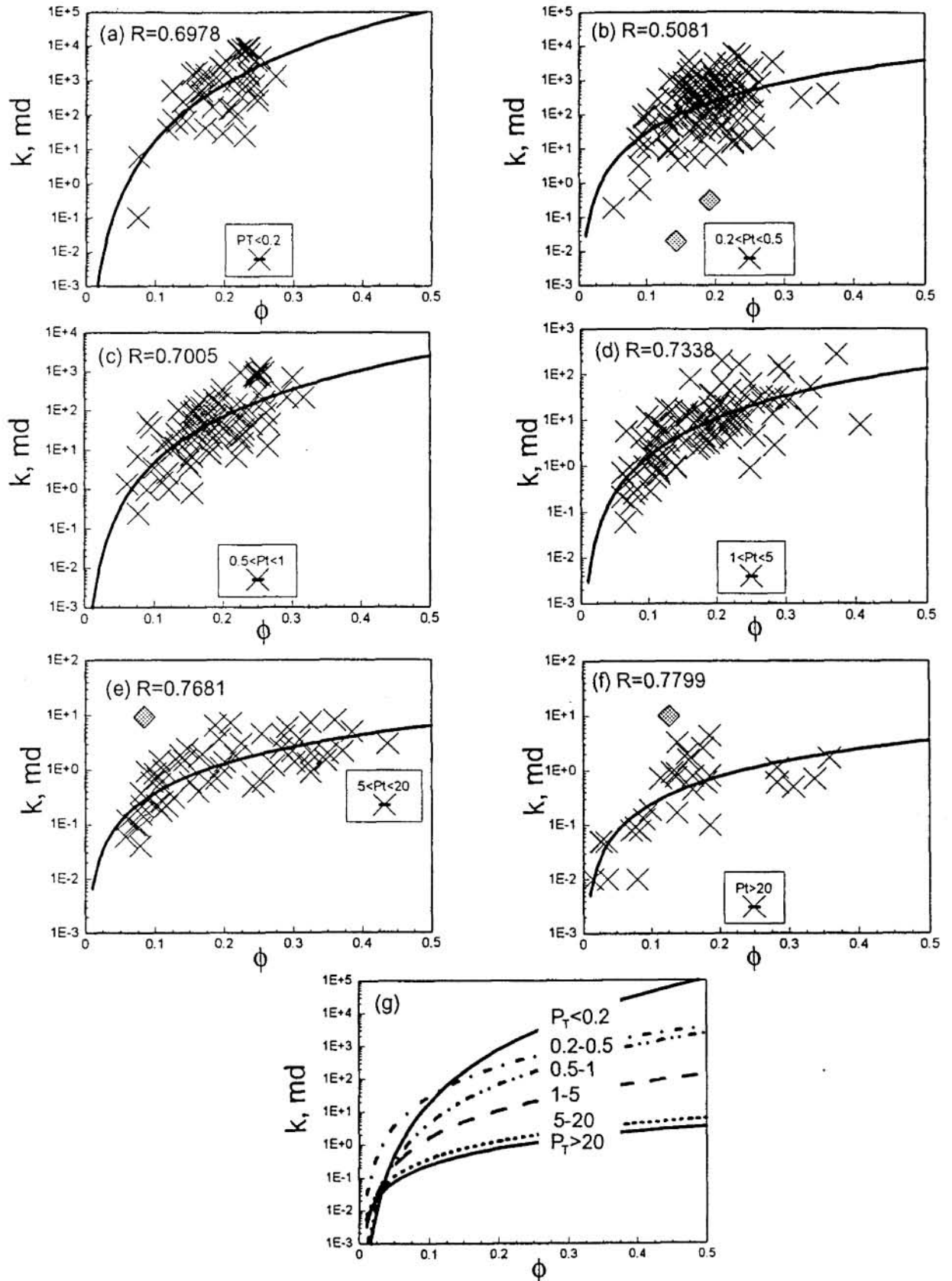


Fig. 5 Correlation between permeability and porosity for data set with (a) $P_T < 0.2$ bar, (b) $0.2 \text{ bar} < P_T < 0.5$ bar, (c) $0.5 \text{ bar} < P_T < 1$ bar, (d) $1 \text{ bar} < P_T < 5$ bar, (e) $5 \text{ bar} < P_T < 20$ bar, (f) $0.2 \text{ bar} < P_T$. A summary of the correlations is shown in (g). (\diamond : data excluded.)

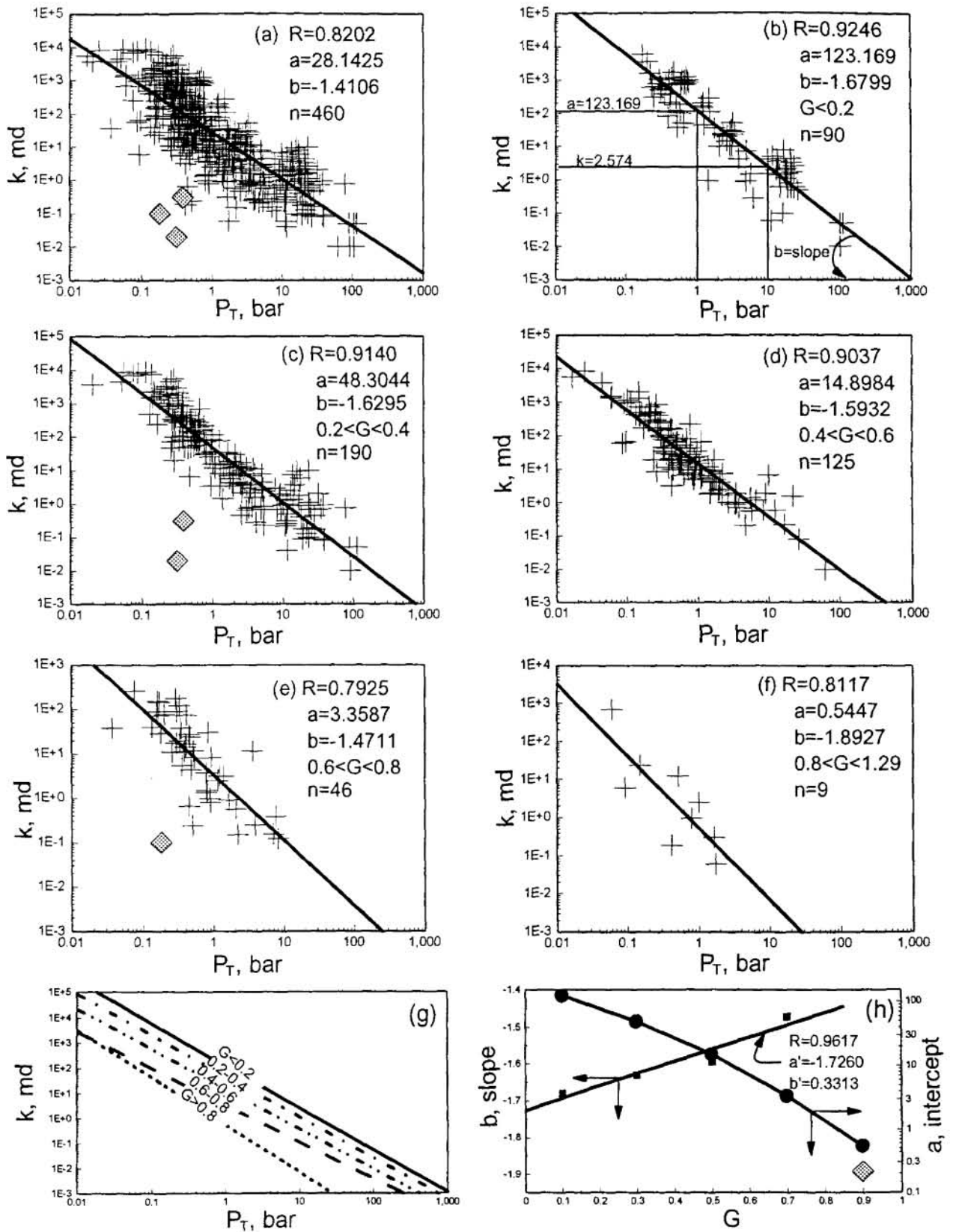


Fig. 6 Correlations between permeability and threshold pressure. (a) for the whole 463 data set and for the data (b) with $G<0.2$, (c) with $0.2<G<0.4$, (d) with $0.4<G<0.6$, (e) $0.6<G<0.8$, and (f) with $G>0.8$. (g) Effect of pore structure factor, G , on k - P_T correlations and (h) The slope and intercept of k - P_T correlations vs G . (◇ : data excluded.)

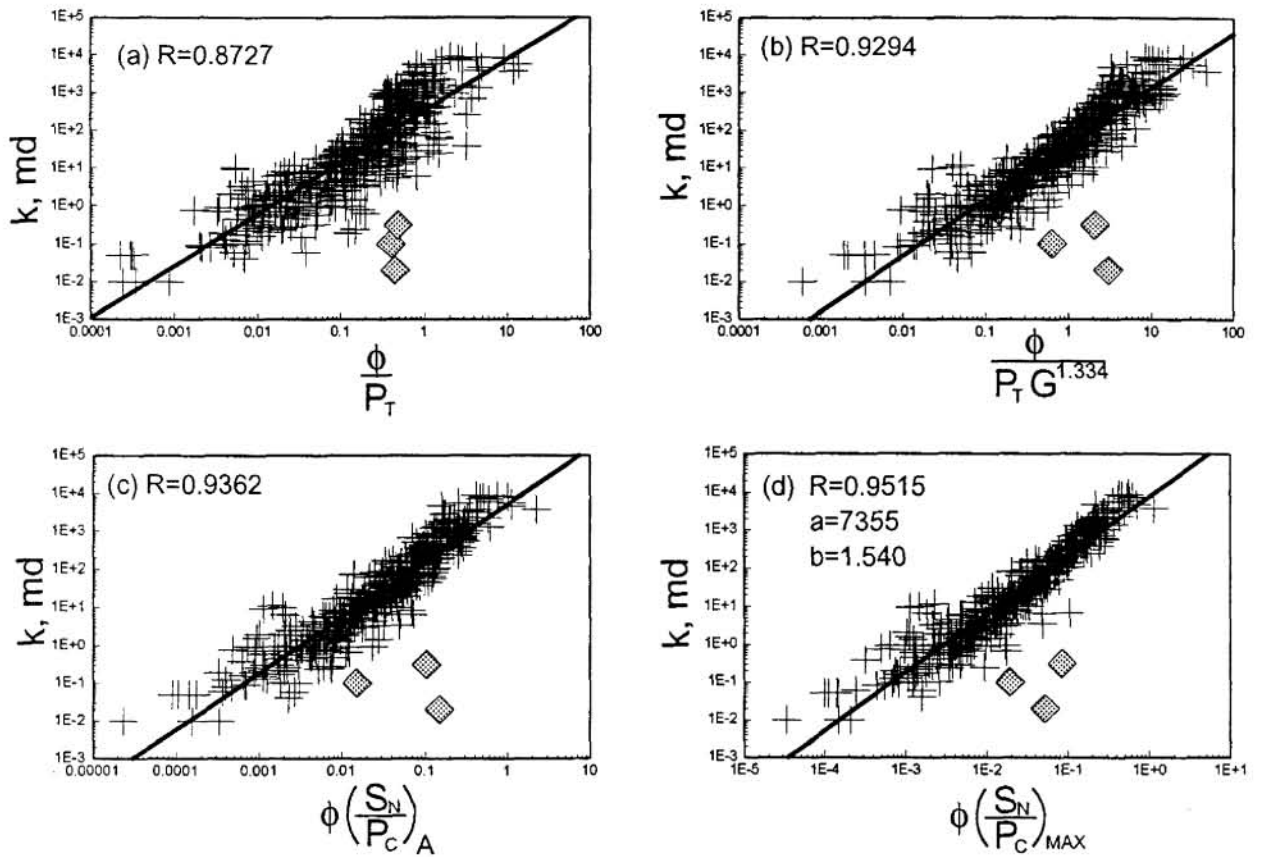


Fig. 7 Correlation between permeability and (a) ratio of porosity to threshold pressure, (b) the Thomeer parameter, (c) the analytical Swanson parameter, and (d) the Swanson parameter for the 463 data set. (◆: data excluded.)

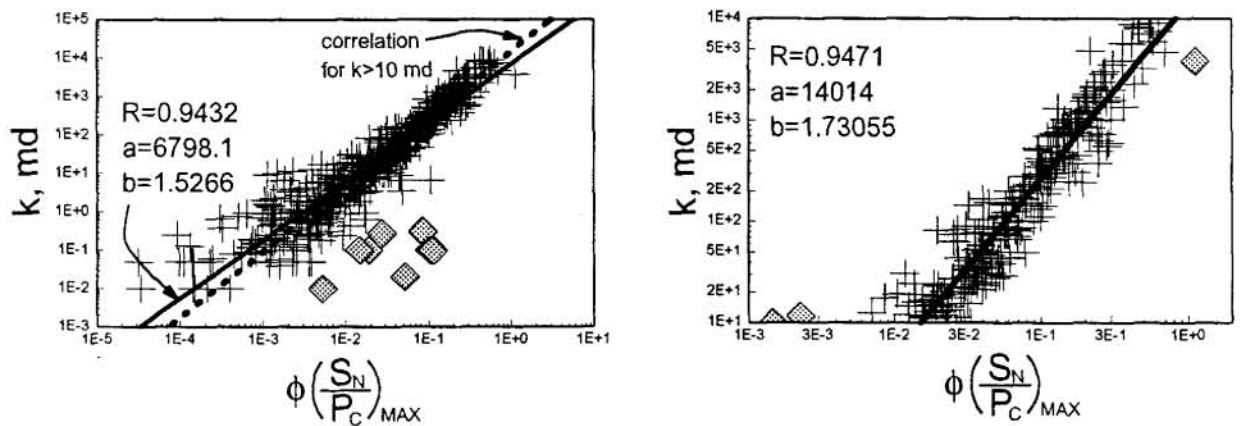


Fig. 8 Correlation between permeability and Swanson parameter for (a) data set of 578 core samples and (b) data with $k > 10$ md. (◆: data excluded.)